

Short-time distribution of particle displacements due to swimming microorganisms

Jean-Luc Thiffeault*

*Department of Mathematics, University of Wisconsin – Madison,
480 Lincoln Dr., Madison, WI 53706, USA*

The experiments of Leptos *et al.* [*Phys. Rev. Lett.* **103**, 198103 (2009)] show that the displacements of small particles affected by swimming microorganisms achieve a non-Gaussian distribution, which nevertheless scales diffusively. We use a simple model where the particles undergo repeated ‘kicks’ due to the swimmers to explain the shape of the distribution as a function of the volume fraction of swimmers. The net displacement is determined by the self-convolution of the drift function caused by one swimmer, and by a Poisson distribution for the frequency of interactions. The only adjustable parameter is the strength of the stresslet term in our spherical squirmer model. The effective diffusivity predicted by the model is consistent with the experiments, with no further parameter adjustments. The diffusive scaling appears to be due to the particular form of the drift function, and is not statistical in origin. The model also suggests that the scaling disappears for longer times, when the swimmers undergo significant reorientation.

I. INTRODUCTION

The study of microswimming has exploded in recent years with the advent of precise, well-controlled experiments. (See for instance the reviews of Pedley and Kessler [1] and Lauga and Powers [2].) This has uncovered a plethora of fascinating behavior, for example the complex interaction of microswimmers with boundaries [3–8], or the spontaneous alignment at high concentrations of ‘pushers,’ organisms whose propulsion mechanism is at the rear [9–15].

Another fruitful research direction is biogenic mixing, or biomixing for short. Does the swimming motion of swimmers influence the effective diffusivity of passive scalars advected by the fluid, such as the nutrients the organisms depend on? This has been proposed as a mixing mechanism in the ocean [16–24], though its effectiveness is still very much open to debate [25–28]. Biomixing has also been studied in suspensions of small organisms [29–32].

The main ingredient in formulating a theory for the enhanced diffusion due to swimming organisms is the *drift* caused by the swimmer [33–35]. Katija and Dabiri [19] and Thiffeault and Childress [22] proposed that the enhanced diffusivity is due to the repeated displacements induced by a swimmer on a particle of fluid. Thiffeault and Childress [22] and Lin *et al.* [36] formulated a probabilistic model where, given the drift caused by one swimmer, an effective diffusivity could be computed. This model has been tested in numerical experiments [37, 38] and modified to include curved trajectories [39] and confined environments [40]. The drift caused by individual microswimmers has also been studied in its own right [41, 42].

* jeanluc@math.wisc.edu

The studies mentioned above have typically been concerned with the effective diffusivity induced by the swimmers, but one can also ask more detailed questions about the distribution of displacements of fluid particles. Wu and Libchaber [43] studied the displacement of spheres larger than the swimming organisms. More recently, Leptos *et al.* [44] studied the microscopic algae *Chlamydomonas reinhardtii*. They used spheres that are much smaller than the organisms, so their distributions can be taken to be close to the displacements of idealized fluid particles. The probability density function (PDF) of tracer displacements was found to be strongly non-Gaussian, though the distributions scaled ‘diffusively’: the distributions collapsed onto each other if rescaled by their standard deviation.

In the present paper we use the model of Thiffeault and Childress [22] and Lin *et al.* [36] to explain the experimental results of Leptos *et al.* in detail. In Section II we give a brief summary of their experiments and of our main results. Section III is devoted to counting the ‘interactions’ of the swimmers with a target fluid particle. In Section IV we combine the distribution of interactions with the displacement induced by the swimmer to obtain the distribution of displacements as a function of time. We use numerical simulations of a single model swimmer (of the squirmer type [8, 45–48]) in Section V to obtain a distribution of displacements which we match to the experiments of Leptos *et al.* The agreement is excellent, in spite of the differences between the model swimmer and the experiments. We discuss our results as well as future directions in Section VII.

II. DESCRIPTION OF EXPERIMENTS AND SUMMARY OF RESULTS

In their experiments Leptos *et al.* [44] use the microorganism *C. reinhardtii*, an alga of the ‘puller’ type, since its two flagella are frontal. This organism has a roughly spherical body with radius $\ell \approx 5 \mu\text{m}$. They observe a distribution of swimming speeds but there is a strong peak around $100 \mu\text{m/s}$. They place fluorescent microspheres of about a micron in radius in the fluid, and optically measure the displacement of the microspheres as the organisms move. The volume fraction of organisms varies from $\phi = 0\%$ (pure fluid) to 2.2% .

They measure the displacement of the microspheres along a reference direction, arbitrarily called x (the system is assumed isotropic). We denote by X_t a random displacement after waiting a time t .¹ Observing many microspheres allows them to compute the probability density function (PDF) of tracer displacements X_t , which we will denote $\rho_{X_t}(x)$. (They write their density $P(\Delta x, \Delta t)$, where $(\Delta x, \Delta t)$ are the same as our (x, t) .) Thus, $\rho_{X_t}(x) dx$ is the probability of observing a particle displacement $X_t \in [x, x + dx]$ after waiting a time t .

At zero volume fraction ($\phi = 0$), the PDF $\rho_{X_t}(x)$ is Gaussian, due solely to thermal noise. For higher number densities, Leptos *et al.* see exponential tails appear and the Gaussian core broaden. The distribution is well-fitted by the sum of a Gaussian and an exponential:

$$\rho_{X_t}(x) = \frac{1-f}{\sqrt{2\pi\delta_g^2}} e^{-x^2/2\delta_g^2} + \frac{f}{2\delta_e} e^{-|x|/\delta_e}. \quad (1)$$

They observe the scalings $\delta_g \approx A_g t^{1/2}$ and $\delta_e \approx A_e t^{1/2}$, where A_g and A_e depend on ϕ . Eckhardt and Zammert [49] have fitted these distributions very well to a continuous-time random walk model, but this does not suggest a mechanism.

¹ We follow the convention that random variables are denoted by uppercase letters, and particular realizations of a random variable are denoted by lowercase letters. Thus the random variables X, A, B, Ψ can have particular values x, a, b, ψ .

The question is, what causes the non-Gaussian form (1)? As was pointed out by Pushkin and Yeomans [40], the experiments are run for a very short time. In Section III we discuss an estimate of ‘interactions’ between swimmers and a target particle. We find that at the highest volume fractions considered in the experiment, the expected number of interactions $\langle M_t \rangle$ with a target particle is

$$\langle M_t \rangle \lesssim .004 \times (R/1 \mu\text{m})^2 + 0.0002 \times (R/1 \mu\text{m})^3. \quad (2)$$

An interaction (or encounter) is defined as a swimmer coming a distance R from the particle during the experiments, taking here to last 0.30 s (the longest experimental run reported). The two terms in (2) correspond to a swimmer passing near a particle during its run (first term), or starting or ending its run near a particle (second term). For $R = 10 \mu\text{m}$ (a value suggested in [44] for significant displacement by a swimmer), we obtain $\langle M_t \rangle \lesssim 0.6$. Hence, a typical fluid particle feels *very few* near-encounters with any swimmer. In order for the central limit theorem to apply, the net displacement must be the sum of many independent displacements, and this is clearly not the case here for the larger values of the displacement. We expect a Gaussian core (due to the many small displacements a particle feels) but non-Gaussian tails (due to the rarity of large displacements).

A key formula derived in Section IV A relates the probability density of X_m , the particle displacement after m encounters, to that of X_t , the displacement after time t :

$$\rho_{X_t}(x) = \sum_{m=0}^{\infty} \rho_{X_m}(x) \mathbb{P}\{M_t = m\}, \quad (3)$$

where $\mathbb{P}\{M_t = m\}$ is the probability of having m encounters (interactions) after a time t . It is a standard result of probability theory that $\mathbb{P}\{M_t = m\}$ is a Poisson distribution (in the limit of infinite volume). Since X_m is the sum of independent and identically distributed (i.i.d.) displacements, all distributed like X_1 , the distribution $\rho_{X_m}(x)$ will be obtained by repeated self-convolution of the distribution $\rho_{X_1}(x)$. This distribution is derived in Section IV C from a suitable average of the *drift function*, $\Delta_\lambda(a, b)$, which measures the net displacement of a fluid particle due to an organism swimming along a path of length λ . The impact parameters a and b describe the geometry of an encounter.

All the ingredients are now in place to compare theory to experiments, except for a model of the swimmer. In Section V we take a ‘squirmers’ [8, 45–48], a spherical swimmer that moves by imposed tangential velocities at its surface (Fig. 4). All the physical parameters are taken from Leptos *et al.* [44], except one: the dimensionless relative strength β of the stresslet term in the squirmer streamfunction (31). This single numerical parameter is chosen to get a good fit with the PDFs from [44]. However, we find increased confidence in the model by then using this fitted value of $\beta = 0.6$ in the formula for effective diffusivity introduced in Thiffeault and Childress [22] and modified for squirmers in [36, 39]:

$$D/\phi = \frac{1}{2} \beta^2 U \ell \approx 90 \mu\text{m}^2/\text{s}. \quad (4)$$

Here $U \approx 100 \mu\text{m}/\text{s}$ is the swimming velocity, $\ell \approx 5 \mu\text{m}$ is the swimmer radius, and ϕ is the volume fraction of swimmers. The corresponding value measured by Leptos *et al.* is $81.3 \mu\text{m}^2/\text{s}$, an excellent agreement given the idealized model and the rough parameter values used. We reiterate the main point: by fitting a single parameter, we reproduce the volume-fraction dependence of the distributions (including non-Gaussian tails, see Fig. 6)

and of the effective diffusivity. This strongly suggests that even though the squirmer model is different from the actual swimmer, the actual mechanism that creates the distributions is present.

Finally, in Section VI we comment on the ‘diffusive scaling’: the fact that the displacement PDFs for different times collapse onto each other after being rescaled by their standard deviation. This phenomenon is remarkably robust: we observe it in our numerical calculations for much longer times than Leptos *et al.* [44], though still not allowing for reorientation of the organisms. We find the root cause is that the PDF $\rho_{X_1}(x)$ for a *single encounter* itself satisfies a diffusive scaling. This means that the scaling is not truly statistical in origin: it simply happens that a single encounter with a swimmer, integrated over space, satisfies such a scaling, at least for our model swimmer and evidently for *Chlamydomonas reinhardtii*. Whether anything more profound is happening is still open to debate. However, when we allow for reorientation (when the organisms are allowed to turn a few times during the experiment), the diffusive scaling apparently disappears (Section VII).

III. COUNTING INTERACTIONS

Our goal is to derive the PDF of displacements $\rho_{X_t}(x)$ from a simple model. We use the model described by Thiffeault and Childress [22] and improved by Lin *et al.* [36], which in spite of its simplicity captures the important features observed in experiments. The first step is to count ‘interactions’ or ‘encounters’: events where a swimmer comes near enough a target particle to significantly displace it.

A. Hitting the interaction sphere

We assume there are N swimmers in a volume V , so the number density of swimmers is $n = N/V$. Initially, each swimmer travels at a speed U in a uniformly random direction. They keep moving along a straight path for a time τ , so that each traces out a segment of length $\lambda = U\tau$. After this a new direction is chosen randomly and uniformly, and the process repeats — each swimmer again moves along a straight path of length λ . Though far from realistic, this model captures many essential features of the system, as found by [22, 36] and as we’ll explore further in this paper.

We wish to follow the displacement of an arbitrary ‘target fluid particle.’ We assume the system to be isotropic and homogeneous, so the choice of fluid particle is immaterial. The swimmers are all simultaneously affecting this fluid particle, but in practice only the closest swimmers significantly displace it. It is thus convenient to introduce an imaginary ‘interaction sphere’ of radius R centered on the target fluid particle, and count the number M_t of ‘interactions,’ that is the number of times a swimmer enters this sphere. (Our treatment applies to two-dimensional systems simply by changing ‘sphere’ to ‘disk’ and ‘volume’ to ‘area.’) Figure 1 illustrates the situation.

Each time a swimmer enters the interaction sphere, the target particle is displaced by some distance. We will address this in the next section and see how to sum the displacements due to many swimmers to obtain the distribution of the net displacement X_t . For now, let us find the distribution of M_t , the number of times a swimmer crosses the interaction sphere during a time t .

The probability that the swimmer starts inside a small volume dV is dV/V , where V

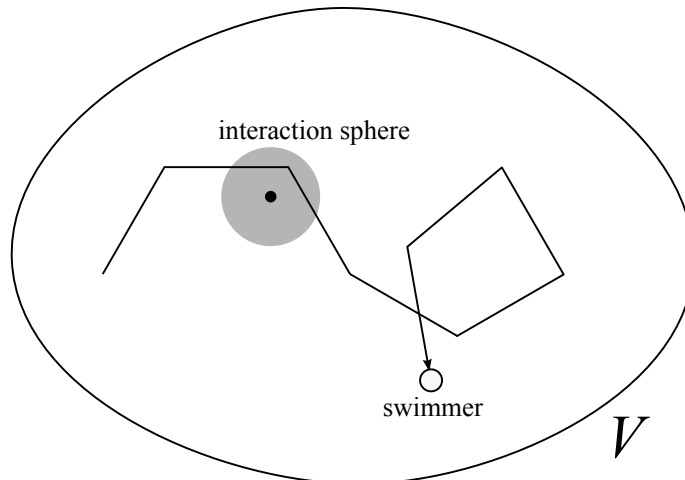


FIG. 1. A swimmer moving inside a volume V along a series of straight paths, each of length λ and in a uniform random direction. The interaction sphere around the target particle (black dot) is shown in gray. Here the swimmer ‘interacts’ twice with the target particle, since two of its paths intersect the sphere.

is the total volume. The probability of a swimmer actually starting inside the interaction sphere is then $V_{\text{sph}}(R)/V$, where $V_{\text{sph}}(R)$ is the volume of a sphere of radius R . (We assume the interaction sphere fits completely within the volume V .) We define the event

$$\mathcal{H}_t = \text{a swimmer crosses the interaction sphere once during time } t < \tau (= \lambda/U), \quad (5)$$

that is, the center of the swimmer is inside the interaction sphere at some point while traveling on a straight path of length $Ut < \lambda$, where U is the uniform speed of a swimmer. To determine the probability of \mathcal{H}_t , observe that because of the homogeneity and isotropy of the swimmers this probability is proportional to the volume swept out by the interaction sphere if it moves a distance Ut , with $0 \leq t < \tau$:

$$p_t := \mathbb{P}(\mathcal{H}_t) = V_{\text{swept}}(R, Ut)/V, \quad V_{\text{swept}}(R, \lambda) := V_{\text{cyl}}(R, \lambda) + V_{\text{sph}}(R), \quad (6)$$

where

$$V_{\text{cyl}}(R, \lambda) := \begin{cases} 2R\lambda, & (2\text{D}); \\ \pi R^2\lambda, & (3\text{D}); \end{cases} \quad V_{\text{sph}}(R) := \begin{cases} \pi R^2, & (2\text{D}); \\ \frac{4}{3}\pi R^3, & (3\text{D}); \end{cases} \quad (7)$$

are respectively the volume of a cylinder of radius R and length λ , and the volume of the interaction sphere. The ratio $V_{\text{sph}}(R)/V$ gives the probability that a swimmer starts inside the interaction sphere. This assumes that the interaction sphere does not intersect the boundary of V .

For N swimmers, let M_t be the total number of interactions with the sphere during time t . In Appendix A we find the probability distribution of M_t :

$$\langle M_t \rangle = n \{V_{\text{swept}}(R, \lambda) (t/\tau) + V_{\text{sph}}(R)\} \quad (8)$$

where $n = N/V$ is the number density of swimmers. In this form we can take the limits $N \rightarrow \infty$ and $V \rightarrow \infty$ while keeping n constant, which doesn’t change the expectation value. Note that we do not assume that the swimmers are ‘synchronized’: though they all

turn at regular intervals τ , each swimmer has its own clock uncorrelated with the other swimmers.

Also from Appendix A, the variance of M_t is

$$\text{Var } M_t = \begin{cases} N \{p_t(1-p_t) + p_0(1-p_0)(t/\tau) + \frac{1}{3}(V_{\text{cyl}}(R, Ut)/V)^2(t/\tau)\}, & t < \tau; \\ N \{p_\tau(1-p_\tau)(t/\tau) + p_0(1-p_0) + \frac{1}{3}(V_{\text{cyl}}(R, \lambda)/V)^2\}, & t \geq \tau. \end{cases} \quad (9)$$

Any term in (9) quadratic in V_{cyl} or p_t will vanish as $V \rightarrow \infty$, and we are left with

$$\text{Var } M_t \simeq \langle M_t \rangle, \quad V \rightarrow \infty. \quad (10)$$

When Nt/τ is large and p_τ is small, as is usually the case in experiments (large volume, many organisms), the distribution of M_t is well approximated by a Poisson distribution:

$$\mathbb{P}\{M_t = m\} \simeq \frac{1}{m!} \langle M_t \rangle^m e^{-\langle M_t \rangle}, \quad Nt/\tau \gg 1, \quad p_\tau \ll 1. \quad (11)$$

For large $\langle M_t \rangle$ we expect that a typical value of M_t will be very close to the mean, since $\langle M_t \rangle / \sqrt{\text{Var } M_t}$ is small. In that case, the central limit theorem applies (M_t is the sum of i.i.d. random variables) and we have the Gaussian approximation

$$\mathbb{P}\{M_t = m\} \simeq \frac{1}{\sqrt{2\pi \text{Var } M_t}} e^{-(m - \langle M_t \rangle)^2 / 2 \text{Var } M_t}, \quad \langle M_t \rangle \gg 1, \quad (12)$$

with $\langle M_t \rangle$ defined in (8).

The mean and variance equations (8) and (9) are exact as long as the interaction sphere is more than a path length λ away from the boundary of V . Equation (11) is valid when there are either many organisms or we wait a long time, and the total volume is large compared to the interaction sphere. Equation (12) further requires $\langle M_t \rangle \gg 1$, which typically happens for long times. We shall not use this last approximation, since the times considered in the experiments are quite short.

B. Interactions in the experiment

Let us now consider these probabilities within the context of the *Leptos et al.* experiments. The velocity of the swimmers is peaked at around $U = 100 \mu\text{m/s}$. Their volume fraction is less than 2.2%. Assuming spherical organisms of radius $\ell = 5 \mu\text{m}$, this gives a number density $n \lesssim 4.2 \times 10^{-5} \mu\text{m}^{-3}$. The maximum observation time is $t = 0.3 \text{ s}$, so that a typical swimmer moves by a distance $Ut = 30 \mu\text{m}$. Using (8) and (7), we then have

$$\langle M_t \rangle \lesssim (4.2 \times 10^{-5} \mu\text{m}^{-3}) \{ \pi R^2 \times (30 \mu\text{m}) + V_{\text{sph}}(R) (t/\tau + 1) \}. \quad (13)$$

In an experiment t/τ is not very well defined (it is the number of times an organism ‘turns’), but in the *Leptos et al.* experiments the swimmers travel in fairly straight lines over the course of the experiments. (Their Fig. 1(a) is for a full second of motion.) Thus, we neglect t/τ and find

$$\langle M_t \rangle \lesssim .004 \times (R/1 \mu\text{m})^2 + 0.0002 \times (R/1 \mu\text{m})^3. \quad (14)$$

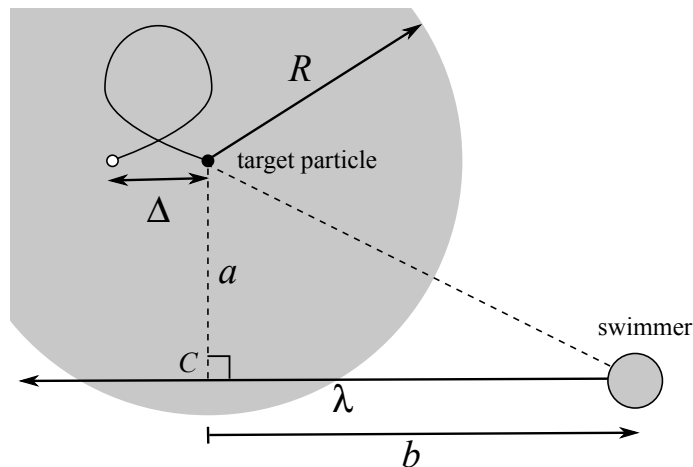


FIG. 2. Definition of impact parameters a and b , displacement $\Delta = \Delta_\lambda(a, b)$, and swimming path length λ . In this picture the parameter b is positive; negative b corresponds to the swimmer starting its trajectory past the point C of smallest initial perpendicular distance to the line of motion. The filled dot is the initial position of the target particle and the hollow dot is its final position after the swimmer has moved by a distance λ . The ‘interaction sphere’ of radius R is also shown. (After Lin *et al.* [36].)

Leptos *et al.* infer an effective range $R_{\text{eff}} \approx 10 \mu\text{m}$ over which advective displacements caused by a swimmer are substantial. Hence, for $R = 10 \mu\text{m}$ (an interaction sphere with a radius twice the swimmer’s), we have $\langle M_t \rangle \lesssim 0.6$. This is at the highest densities used in the experiments. We conclude that a typical fluid particle is only strongly affected by about one swimmer. The only displacements that a particle feels ‘often’ are the very small ones due to all the faraway swimmers. We thus expect the displacement PDF to have a central Gaussian core (since the central limit theorem will apply for the small displacements), but strongly non-Gaussian tails. This is what is observed, and we will spend the remainder of the paper making this more precise.

IV. THE DISTRIBUTION OF DISPLACEMENTS

Now that we’ve examined how often swimmers interact with a sphere of radius R centered around a target particle (Section III), we will look at how the particle gets displaced. This is a problem of probability: we must combine the probability of an interaction together with the probability of particular displacements values to obtain the distribution of displacements as a function of time.

A. Summing displacements

Figure 2 shows the setup of an interaction. Since the system is homogeneous and isotropic, only two ‘impact parameters’ a and b are needed to describe an interaction. (The swimmer also needs to be axisymmetric about its swimming direction, which is not true for *C. reinhardtii* but will hold for our model swimmer.) These are depicted in the figure: here C is the point along the line of motion that is closest to the initial position of the particle, and

$a \in [0, R]$ is this closest distance. The parameter $b \in [-R, \lambda + R]$ is the distance from C to the initial position of the swimmer. A negative value of b means the swimmer started its path beyond the point C . The parameter λ is the total path length of swimming, assuming a straight swimming path.

Following Lin *et al.* [36], we start from the drift function $\Delta_\lambda(a, b)$ induced by a single swimmer. Each time a swimmer enters the interaction sphere we have an encounter, which causes a displacement of the target particle. (We use ‘encounter’ and ‘interaction’ interchangeably.) Thus, after m encounters, the total random displacement in the x direction is²

$$X_m = \sum_{k=1}^m \Delta_\lambda(A_k, B_k) \cos \Psi_k \quad (15)$$

where each encounter has random i.i.d. impact parameters (A_k, B_k) and angle Ψ_k . (A_k and B_k are not generally independent from each other.) The $\cos \Psi_k$ term is a projection of an arbitrary direction onto the x axis. We select the x displacement here, but by isotropy the statistics in any direction are the same.

We distinguish between X_m , a random variable giving the displacement of a particle after m encounters, and $X_t \equiv X_{M_t}$, a random variable giving the displacement of a particle after time t . The latter involves a random number M_t of encounters. The probability density of X_m can be related to that of X_t , the x displacement after a time t , by first observing that $\mathbb{P}\{X_m \in [x, x + dx]\} = \mathbb{P}\{X_t \in [x, x + dx] \mid M_t = m\}$,³ and

$$\begin{aligned} \mathbb{P}\{X_t \in [x, x + dx]\} &= \sum_{m=0}^{\infty} \mathbb{P}\{X_t \in [x, x + dx], M_t = m\} \\ &= \sum_{m=0}^{\infty} \mathbb{P}\{X_t \in [x, x + dx] \mid M_t = m\} \mathbb{P}\{M_t = m\}, \end{aligned} \quad (16)$$

where $\mathbb{P}\{M_t = m\}$ is the probability of getting m encounters in time t , derived in Section III A. In terms of densities, Eq. (16) reads

$$\rho_{X_t}(x) = \sum_{m=0}^{\infty} \rho_{X_m}(x) \mathbb{P}\{M_t = m\}, \quad (17)$$

where $\rho_{X_t}(x) = \mathbb{P}\{X_t \in [x, x + dx]\}$ and $\rho_{X_m}(x) = \mathbb{P}\{X_m \in [x, x + dx]\}$.

B. PDFs of impact parameters

Next, we derive the probability density functions of the impact parameters. As mentioned in Section IV A we assume that the random variables (A_k, B_k) and Ψ_k in (15) are i.i.d. for different k . The random angle of swimming Ψ_k is independent of (A_k, B_k) , but the latter pair will depend on each other. The probability densities are thus written $\rho_\Psi(\psi)$ and $\rho_{AB}(a, b)$.

Because of isotropy, the angular variables have simple densities:

$$\rho_\Psi(\psi) = 1/\pi, \quad (2D); \quad \rho_\Psi(\psi) = \frac{1}{2} \sin \psi, \quad (3D), \quad (18)$$

² The notation should really be $X_{m,\lambda}$ to exhibit the dependence on the path length λ , but we opt for keeping the lighter notation.

³ $\mathbb{P}\{A|B\}$ is the conditional probability of A occurring given that B has occurred; $\mathbb{P}\{A, B\}$ is the joint probability of both A and B occurring.

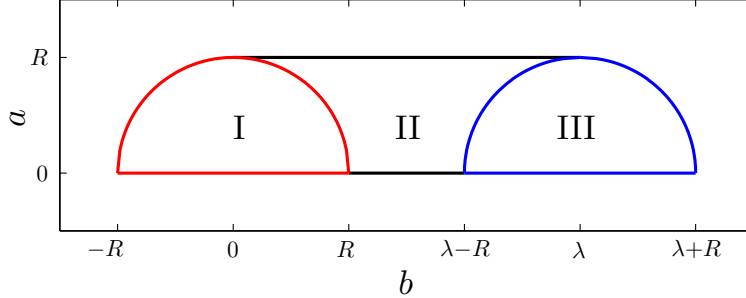


FIG. 3. The domain $\Omega_{ab} = \text{I} \cup \text{II} \cup \text{III}$ of the impact parameters a and b for fixed path length λ (see Fig. 2). Region I corresponds to swimmers that start their path inside the interaction sphere; swimmers in Region II cross the sphere completely; swimmers in Region III finish their path inside the sphere. Note that the figure depicts $\lambda > 2R$, but all the formulas hold for $\lambda < 2R$ as well, when regions I and III overlap because some trajectories both start and finish inside the sphere.

for $\psi \in \Omega_\psi = [0, \pi]$. In two dimensions, the joint density $\rho_{AB}(a, b)$ is uniform over the domain $\Omega_{ab} = \{0 \leq a \leq R, -\sqrt{R^2 - a^2} \leq b \leq \lambda + \sqrt{R^2 - a^2}\}$ depicted in Fig. 3. These are the values of a and b for which a swimmer's straight path intersects the interaction sphere. After normalizing, we find the density

$$\rho_{AB}(a, b) = 2/V_{\text{swept}}(R, \lambda) \quad (2\text{D}). \quad (19)$$

In three dimensions, the domain in Fig. 3 is interpreted as a surface of revolution about $a = 0$, leading to the density

$$\rho_{AB}(a, b) = 2\pi a/V_{\text{swept}}(R, \lambda) \quad (3\text{D}). \quad (20)$$

For both the 2D and 3D cases, $\rho_{AB}(a, b)$ is then normalized such that

$$\int_{\Omega_{ab}} \rho_{AB}(a, b) da db = \int_0^R \int_{-\sqrt{R^2 - a^2}}^{\lambda + \sqrt{R^2 - a^2}} \rho_{AB}(a, b) db da = 1. \quad (21)$$

We can immediately compute some useful quantities, such as the variance $\text{Var } X_t = \langle X_t^2 \rangle - \langle X_t \rangle^2$. From (15), the mean $\langle X_t \rangle$ is zero by isotropy, as reflected by $\int_{\Omega_\psi} \rho_\Psi(\psi) \cos \psi d\psi = 0$. It then follows from (17) that the variance is $\langle X_t^2 \rangle = \langle M_t \rangle \langle X_1^2 \rangle$, or

$$\begin{aligned} \langle X_t^2 \rangle &= \langle M_t \rangle \int_{\Omega_{ab} \times \Omega_\psi} \rho_{AB}(a, b) \rho_\Psi(\psi) \Delta_\lambda^2(a, b) \cos^2 \psi da db d\psi, \\ &= \frac{\langle M_t \rangle}{d} \int_{\Omega_{ab}} \rho_{AB}(a, b) \Delta_\lambda^2(a, b) da db, \end{aligned} \quad (22)$$

where $d = 2$ or 3 is the dimension of space. Equation (22) is $1/d$ times equation (2.2) in Lin *et al.* [36], since x is only one of the d directions of motion. By isotropy, the radial squared-displacement $\langle r^2 \rangle$ is equal to $d \times \langle X_t^2 \rangle$.

C. Distribution of X_m

We are now in a position to compute, at least formally, the distribution of total particle displacements $\rho_{X_m}(x) = \mathbb{P}\{X_m \in [x, x + dx]\}$. Let us first compute the probability density

function of

$$X_1 = \Delta_\lambda(A, B) \cos \Psi, \quad (23)$$

the displacement after one encounter. We have

$$\mathbb{P}\{X_1 > x\} = \int_{\Omega_{ab} \times \Omega_\psi} \rho_{AB}(a, b) \rho_\Psi(\psi) \chi_{\{\Delta_\lambda \cos \psi > x\}}(a, b, \psi) da db d\psi, \quad (24)$$

where χ_Ω is the indicator function of the set Ω , *i.e.*, its value is 1 when its argument is in Ω , and zero otherwise. The ψ integral will be limited by the indicator function, so that

$$\mathbb{P}\{X_1 > x\} = \int_{\Omega_{ab}} \rho_{AB}(a, b) \mathcal{I}(x/\Delta_\lambda(a, b)) da db, \quad (25)$$

where

$$\mathcal{I}(\zeta) = \begin{cases} 1, & \zeta < -1; \\ \int_0^{\cos^{-1}(\zeta)} \rho_\Psi(\psi) d\psi = \begin{cases} \frac{1}{\pi} \cos^{-1}(\zeta), & \text{(2D)} \\ \frac{1}{2}(1 - \zeta), & \text{(3D)} \end{cases} & -1 \leq \zeta \leq 1; \\ 0, & \zeta > 1. \end{cases} \quad (26)$$

The density is recovered by differentiating the cumulative distribution:

$$\rho_{X_1}(x) = -\frac{d}{dx} \mathbb{P}\{X_1 > x\} = -\int_{\Omega_{ab}} \frac{\rho_{AB}(a, b)}{\Delta_\lambda(a, b)} \mathcal{I}'(x/\Delta_\lambda(a, b)) da db. \quad (27)$$

Differentiating (26) gives

$$\rho_{X_1}(x) = \frac{1}{\pi} \int_{\Omega_{ab}} \frac{\rho_{AB}(a, b)}{\sqrt{\Delta_\lambda^2(a, b) - x^2}} \chi_{\{\Delta_\lambda > |x|\}}(a, b) da db, \quad \text{(2D);} \quad (28)$$

and

$$\rho_{X_1}(x) = \frac{1}{2} \int_{\Omega_{ab}} \frac{\rho_{AB}(a, b)}{\Delta_\lambda(a, b)} \chi_{\{\Delta_\lambda > |x|\}}(a, b) da db, \quad \text{(3D).} \quad (29)$$

Oddly enough the expression is more compact for 3D than for 2D. In both cases the indicator function in the integrand says that the displacement $\Delta_\lambda(a, b)$ must be at least $|x|$, but larger displacements can contribute as well because of the angular average. The larger the displacement the *less* likely it is to contribute, since its projection is less likely to be small.

What about the density function for two steps, $\rho_{X_2}(x)$? Since X_2 is the sum of two i.i.d. random variables X_1 , its PDF is just the convolution of $\rho_{X_1}(x)$ with itself:

$$\rho_{X_2}(x) = \int_{-\infty}^{\infty} \rho_{X_1}(x - y) \rho_{X_1}(y) dy =: (\rho_{X_1} * \rho_{X_1})(x). \quad (30)$$

For m steps we have $\rho_{X_m}(x) = (\rho_{X_1} * \dots * \rho_{X_1})(x)$, often written $\rho_{X_m}(x) = \rho_{X_1}^{*m}(x)$.

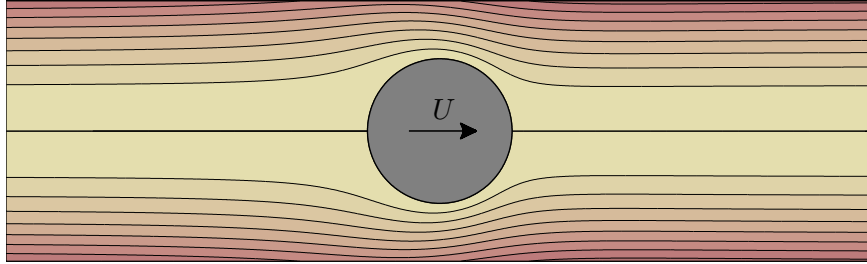


FIG. 4. Contour lines for the axisymmetric streamfunction of a squirmer of the form (31), with $\beta = 0.6$. This swimmer is of the puller type, as for *C. reinhardtii*.

V. NUMERICAL SIMULATIONS

We now compare the theory discussed in the previous sections to the experiments of Leptos *et al.* We shall use a model swimmer of the squirmer type [8, 45–48], with axisymmetric streamfunction [36]

$$\Psi_{\text{sf}}(\rho, z) = \frac{1}{2}\rho^2 U \left\{ -1 + \frac{\ell^3}{(\rho^2 + z^2)^{3/2}} + \frac{3}{2} \frac{\beta \ell^2 z}{(\rho^2 + z^2)^{3/2}} \left(\frac{\ell^2}{\rho^2 + z^2} - 1 \right) \right\} \quad (31)$$

in a frame moving at speed U . Here z is the swimming direction and ρ is the distance from the z axis. To mimic *C. reinhardtii*, we use $\ell = 5 \mu\text{m}$ and $U = 100 \mu\text{m/s}$. We take also $\beta = 0.6$ for the relative stresslet strength, which gives a swimmer of the puller type, just like *C. reinhardtii*. The contour lines of the axisymmetric streamfunction (31) are depicted in Fig. 4. The parameter β is the only one that was fitted to give good agreement later.

First we compute the distributions of displacements for a single encounter. To do so we simulate the displacement of particles to compute the drift function $\Delta_\lambda(a, b)$. We take $\lambda = 12 \mu\text{m}$, since the time is $t = 0.12\text{s}$ in Fig. 2(a) of Leptos *et al.*, and our swimmer moves at speed $U = 100 \mu\text{m/s}$. Once we have $\Delta_\lambda(a, b)$ for a large grid of a and b values, we compute the single-interaction PDF $\rho_{X_1}(x)$ numerically using formula (29). The resulting distribution is shown in Fig. 5 ($m = 1$, narrowest distribution). The distribution has a cutoff for $|x| > \lambda$, since no particles move much further than the swimmer.

To compute $\rho_{X_1}(x)$ we chose a radius $R = 30 \mu\text{m}$ for the interaction sphere. This is capacious enough that the largest displacements are included, but not so large that we need a very high a - b grid resolution to see those large displacements. Note, however, that this value of R is *not* large enough to compute the standard deviation of the PDF accurately, since this is dominated by the cumulation of small faraway displacements. A value of $R \approx 1000 \mu\text{m}$ is more appropriate here, but then the large number of convolutions required is prohibitive (a large-deviation approach is called for). The value of R we chose will still allow us to see the tails clearly. We use a grid with spacing 0.05 in b and 0.008 in $\log a$.

Let us estimate the number of encounters that a particle will have with a swimmer during the time of the experiment. Using (7) and (8), we have for the expected number of encounters

$$\langle M_t \rangle \simeq (1.9 \times 10^{-3} \mu\text{m}^{-3}) \phi \left\{ \pi R^2 \times (12 \mu\text{m}) + \frac{4}{3} \pi R^3 \right\}. \quad (32)$$

We neglected the number of turns t/τ since for such a short experiment the swimmers are mostly moving in one direction, as is apparent from Fig. 1(a) of Leptos *et al.* [44].

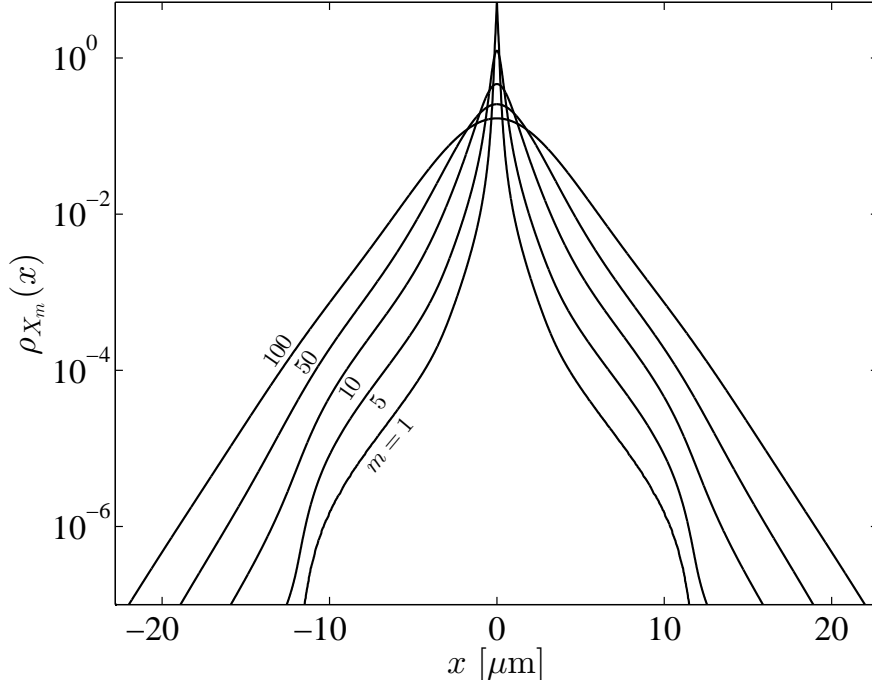


FIG. 5. The PDF $\rho_{X_m}(x)$ of displacements after m interactions with a swimmer. The swimmer here is a spherical squirmer [45, 46] with velocity $U = 100 \mu\text{m/s}$, stresslet strength $\beta = 0.6$ and radius $\ell = 5 \mu\text{m}$. For $m = 1$, there is a cutoff at the swimmer path length $\lambda = 12 \mu\text{m}$.

For $R = 30 \mu\text{m}$ the second term in (32) is larger: since a typical organism does not travel very far, most particles will be influenced by virtue of already being near a swimmer at the start of the experiment. With this value for R , we find $\langle M_t \rangle \approx 281 \phi$. Hence, we expect about 6 encounters when $\phi = 2.2\%$. This is larger than estimated in Section III B, but this is because here we have a larger value of R that includes mostly small displacements.

To compare to Leptos *et al.*, we take a few self-convolutions of $\rho_{X_1}(x)$ with itself, one for each of m encounters, to obtain $\rho_{X_m}(x)$. We then use (11), the probability of having m encounters, into (17) to compute $\rho_{X_t}(x) = \mathbb{P}\{X_t \in [x, x + dx]\}$. We also convolve with a Gaussian distribution of half-width $\sigma = 0.26 \mu\text{m}$ to mimic thermal noise. This follows from the value $D_0 = 0.28 \mu\text{m}^2/\text{s}$ measured by Leptos *et al.* for the diffusivity of the microspheres. The value of D_0 is consistent with the Stokes–Einstein equation for the diffusivity of thermally-agitated small spheres in a fluid.

The results are plotted into Fig. 6(a) and compared to the data of Fig. 21(a) of Leptos *et al.* [44]. The agreement is excellent: we remind the reader that we adjusted only one parameter, $\beta = 0.6$. All the other physical quantities were gleaned from Leptos *et al.* What is most remarkable about the agreement in Fig. 6(a) is that it was obtained using a model swimmer, the spherical squirmer, which is not expected to be such a good model for *C. reinhardtii*. The real organisms are strongly time-dependent, for instance, and do not move in a perfect straight line. Nevertheless the model captures very well the PDF of displacements.

To reinforce the argument that the data agrees with the model with little fitting, let us compute the effective diffusivity due to the swimmers without any further parameter adjustment. The model introduced in Thiffeault and Childress [22] and modified

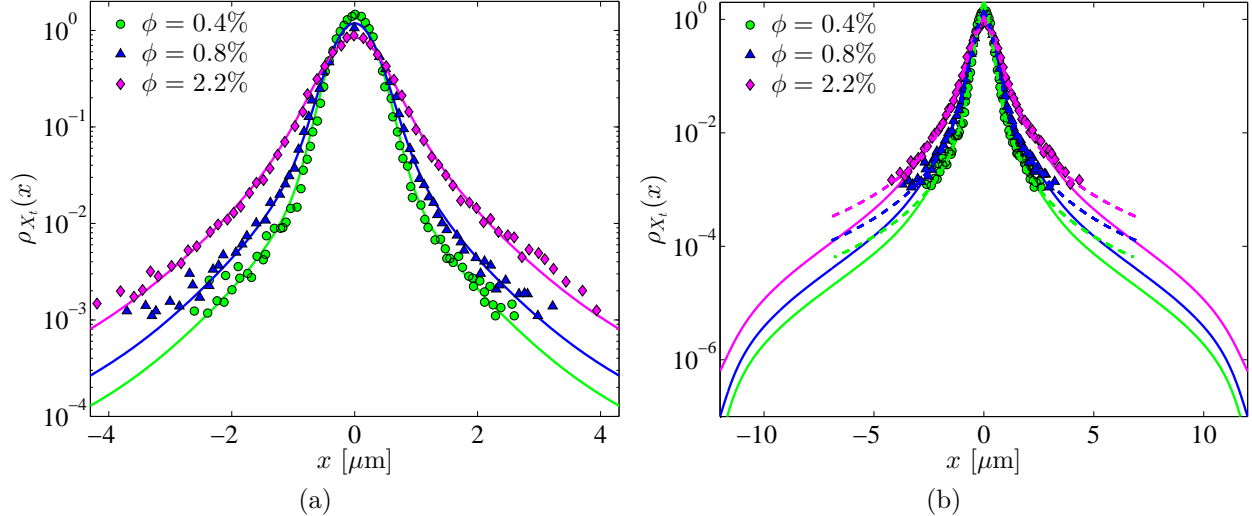


FIG. 6. (a) The PDF of particle displacements after a time $t = 0.12$ s, for several values of the volume fraction ϕ . The data is from Leptos *et al.* [44], and the figure should be compared to their Fig. 2(a). The theoretical curves were obtained by self-convolution of the one-encounter distribution $\rho_{X_1}(x)$ for a model squirmer (Fig. 5), with some noise corresponding to thermal diffusivity. (b) Same as (a) but on a wider scale, also showing the form suggested by Eckhardt and Zammert [49] (dashed lines).

for squirmers in [36, 39] predicts that the effective diffusivity should be roughly $D = \frac{2}{3}\pi\beta^2 U n l^4 = \frac{1}{2}\beta^2 U l \phi$, when transport is dominated by the stresslet term. This gives $D \approx 0.5(0.6)^2(100)(5)\phi \approx (90 \mu\text{m}^2/\text{s})\phi$. In Leptos *et al.*, this coefficient is $81.3 \mu\text{m}^2/\text{s}$, in excellent agreement with 90 given the simplicity of the model and the rough estimation of parameters. (Pushkin *et al.* [42] obtained an estimate of $83 \mu\text{m}^2/\text{s}$ using the swimmer's entrained volume.)

VI. THE DIFFUSIVE SCALING

One of the most remarkable property of the PDFs found by Leptos *et al.* is the *diffusive scaling*. This is illustrated in Fig. 7: the unrescaled displacement PDFs are shown in Fig. 7(a); the same PDFs are shown again in Fig. 7(b), but rescaled by their standard deviation. The PDFs collapse onto a single curve (the earliest time showing the largest deviation). Figure 7 was obtained in the same manner as Fig. 6, using our probabilistic approach. Hence, the diffusive scaling persists in our model. However, in Fig. 7 we left out thermal diffusion completely, showing that it is not needed for the diffusive scaling to emerge.

The diffusive scaling was also observed by Lin *et al.* [36] in direct numerical simulations of squirmers. Here we have the luxury of going much further in time and to examine the probability of larger displacements, since we are simply carrying out integrals and not running a statistically-limited experiment or simulation. (The numerical integrals are of course limited by resolution.) Figure 8 strikingly confirms that the diffusive scaling applies for a very long range, up to a cut-off for each distribution. The tails in Fig. 8(b) validate

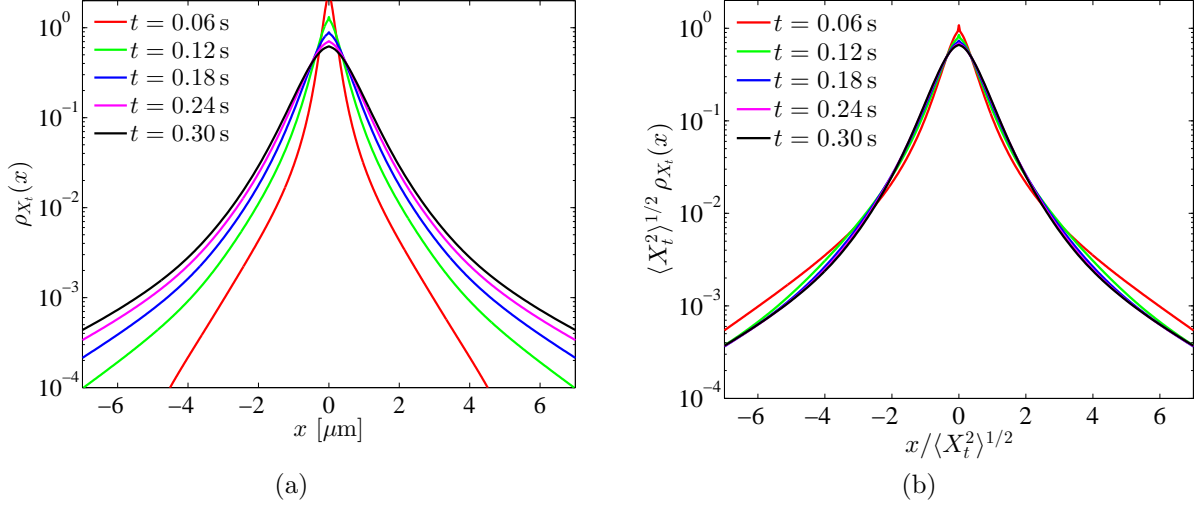


FIG. 7. (a) PDFs of particle displacements for squirmers for different times, at a number density $\phi = 2.2\%$. (b) The same PDFs rescaled by their standard deviation.

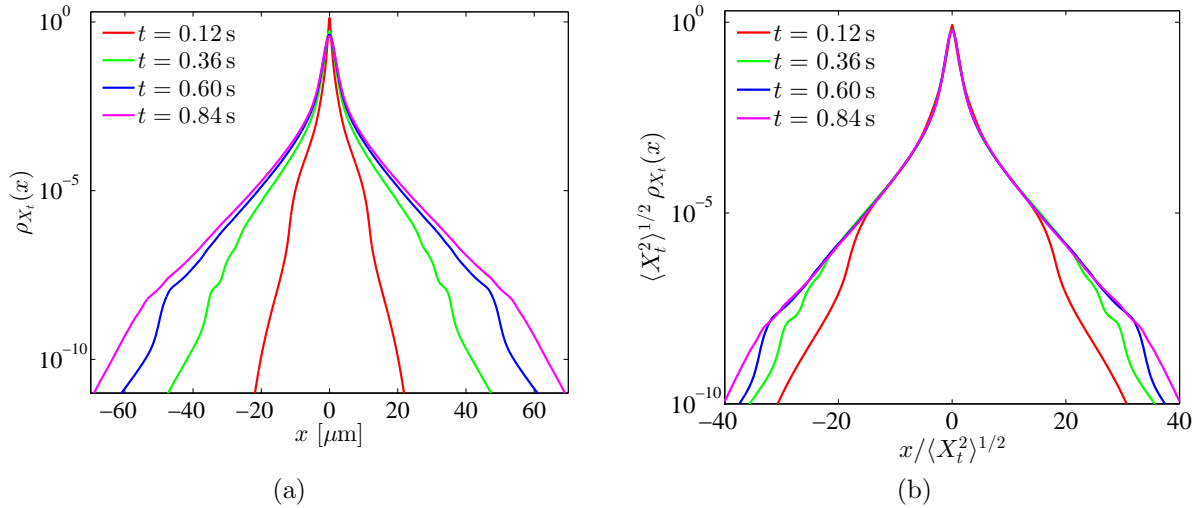


FIG. 8. Same as Fig. 7 but for longer times and with a wider scale.

the Gaussian-with-exponential-tails form (1) suggested by Leptos *et al.*, at least for our squirmer-type microswimmer.

How can we explain the striking scaling observed in Fig. 8? The PDFs shown are for relatively short times, in that a full path length has not been completed. However, the later times are long enough that we can approximate $\mathbb{P}\{M_t = m\} \approx \langle M_t \rangle \delta_{m, \langle M_t \rangle}$ and $\text{Var } X_t \approx$

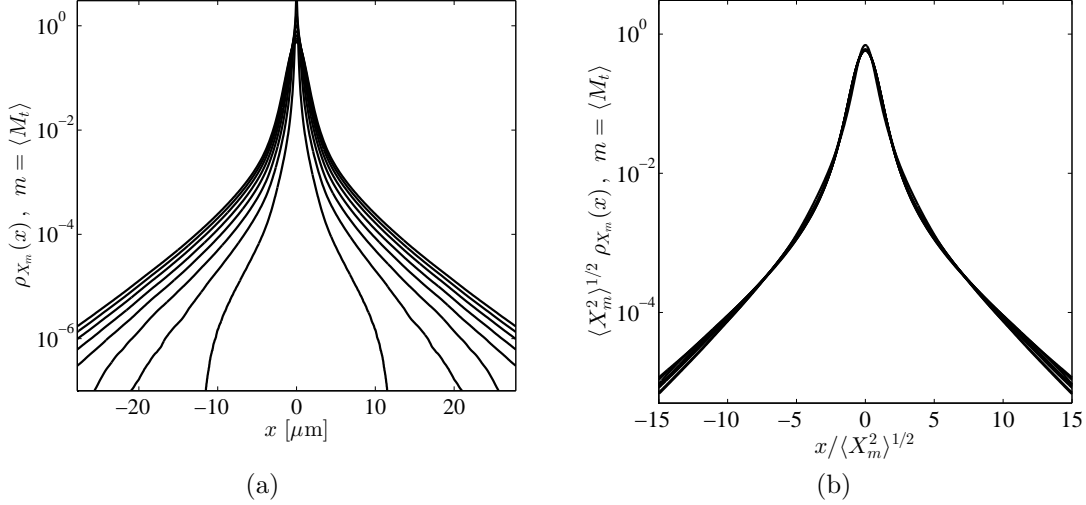


FIG. 9. (a) The PDF of X_m , $\rho_{X_m}(x)$, for $m = \langle M_t \rangle$ and t varying from 0.06 s (narrowest curve) to 0.96 s (broadest) in increments of 0.12 s. (b) The same PDFs but rescaled by their standard deviation.

$\text{Var } X_{\langle M_t \rangle}$. The scaled variable $\Xi_t = X_t / \sqrt{\text{Var } X_t}$ has PDF

$$\begin{aligned} \rho_{\Xi_t}(\xi) &= \sqrt{\text{Var } X_t} \rho_{X_t}(\xi \sqrt{\text{Var } X_t}) \\ &= \sqrt{\text{Var } X_t} \sum_{m=0}^{\infty} \rho_{X_m}(\xi \sqrt{\text{Var } X_t}) \mathbb{P}\{M_t = m\} \\ &\approx \sqrt{\text{Var } X_m} \rho_{X_m}(\xi \sqrt{\text{Var } X_m}) \Big|_{m=\langle M_t \rangle}. \end{aligned}$$

Hence, it is enough for ρ_{X_m} with $m = \langle M_t \rangle$ to satisfy the diffusive scaling. Figure 9 shows that it does.

In fact even the single-encounter PDF, $\rho_{X_1}(x)$, satisfies a diffusive scaling (Fig. 10), though it doesn't appear quite as striking as for the other distributions. In some sense this means the diffusive scaling is not statistical in nature: it has its origin in the distribution of particle displacements due to a *single* swimmer, with no randomness. Exactly how this scaling arises from the exact form of $\Delta_\lambda(a, b)$ is still unclear. In Fig. 11 we show the drift function $\Delta_\lambda(a, b)$ for a path length $\lambda = 96 \mu\text{m}$. How this shape changes as a function of λ , and hence leads to the diffusive scaling, will be the subject of future investigations. Note, however, that even though the variance of X_t is dominated by the far field (stresslet) contribution [36], the tails in $\rho_{X_t}(x)$ are not due to the stresslet term. In fact large displacements, which arise from particles near the organism, cannot be determined by the stresslet term since it ceases to dominate as we approach the organism. This is why we do not observe the x^{-4} scaling of the tails derived by Pushkin and Yeomans [40] for a stresslet. A mechanism similar to the near-body displacements observed for squirmers must instead be at play [36].

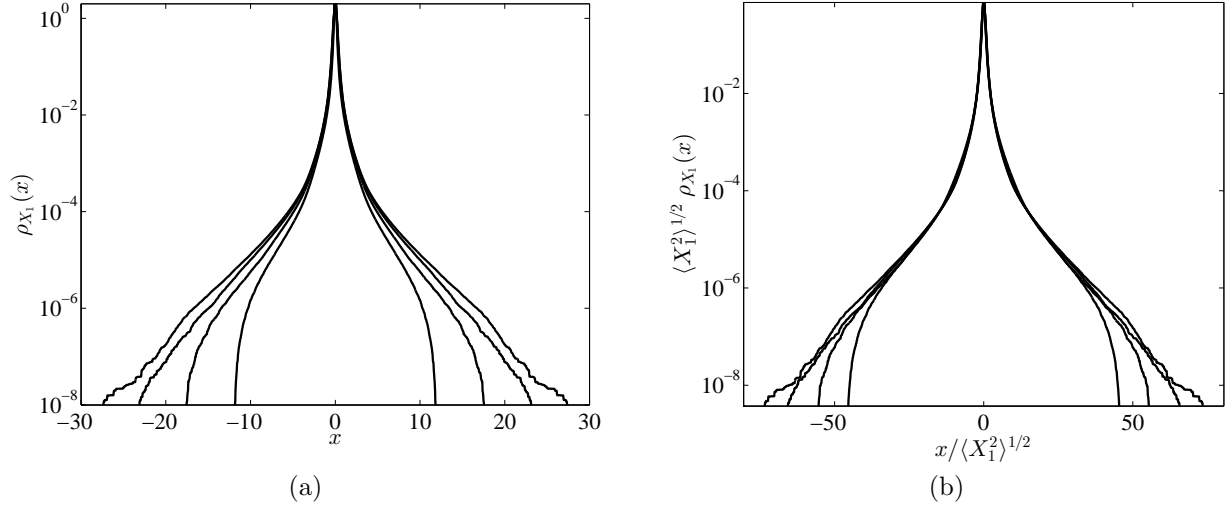


FIG. 10. (a) The PDF of X_1 , $\rho_{X_1}(x)$, for a squirmer swimming a distance $\lambda = Ut$, with t varying from 12s (narrowest curve) to 96s (broadest) in increments of 0.12s. (b) The same PDFs but rescaled by their standard deviation. The largest x values are somewhat noisy, since their small probability is reflected by a very small region of numerical integration.

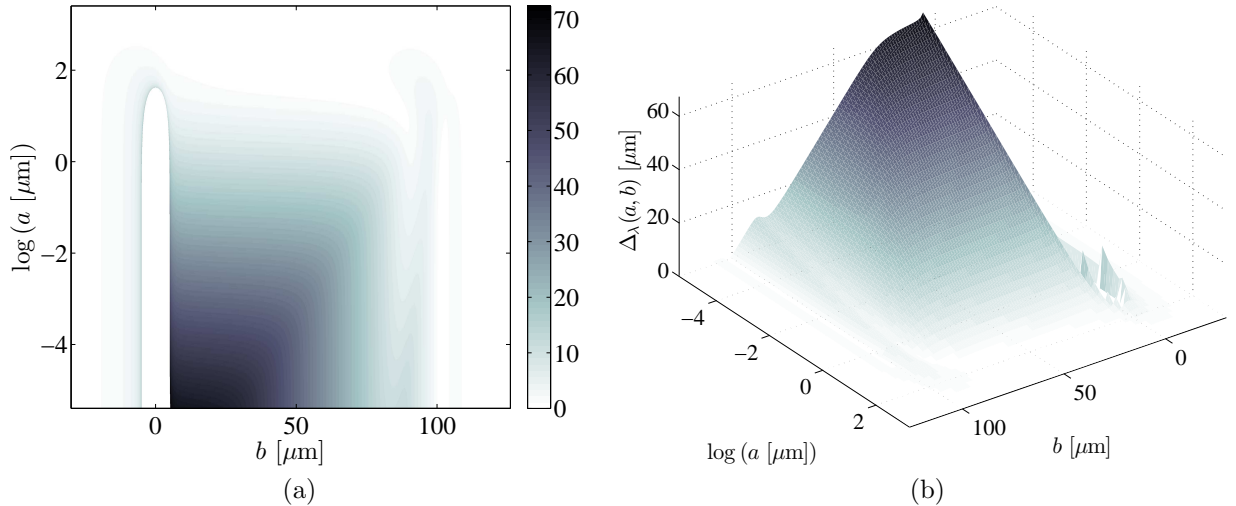


FIG. 11. Drift function $\Delta_\lambda(a, b)$ (in μm) for a swimming path length $\lambda = 96 \mu\text{m}$. In (a), the spherical squirmer's outline appears elongated because of the logarithmic vertical axis. The impact parameters a and b are defined in Fig. 2.

VII. DISCUSSION

Perhaps the most intriguing question is: why does the squirmer model do so well? After all, the real organisms are unsteady, have flagella, do not travel in a straight line, have a distribution of velocities, interact with each other, etc. It seems the ingredient required to get the non-Gaussian tails and the diffusive scaling is contained in a drift function that resembles Fig. 11. Whether the time-dependent organism has such a drift function will be

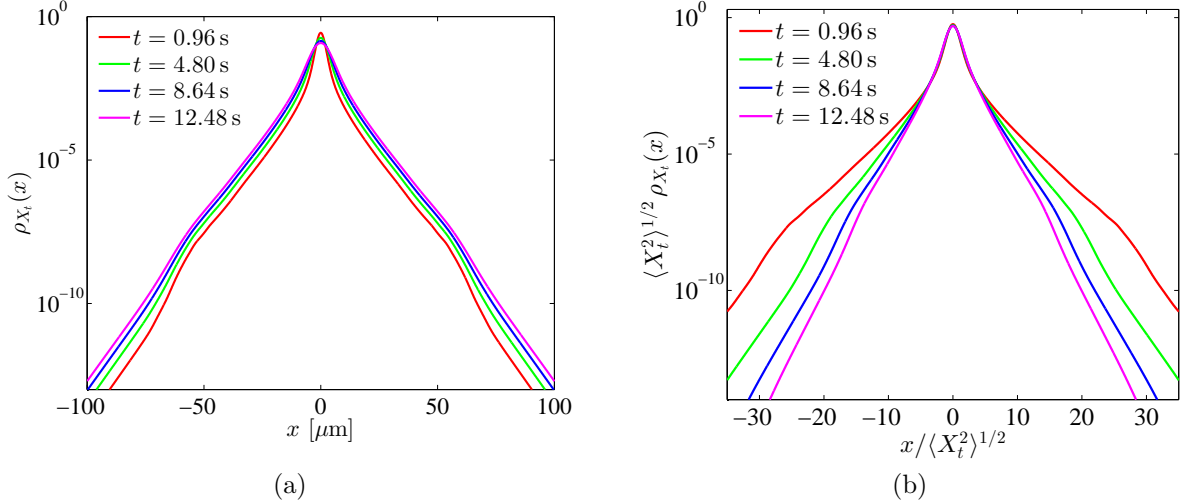


FIG. 12. (a) PDFs of particle displacements for squirmers for different times, at a number density $\phi = 2.2\%$ and a path length $\lambda = 0.96 \mu\text{m}$. Unlike Fig. 8, here the swimmers undergo several path lengths of swimming, with reorientation in between. (b) The same PDFs rescaled by their standard deviation. The PDFs scale diffusively only in their central core. The times shown correspond respectively to 1, 5, 9, and 13 reorientations.

the subject of future investigations.

For longer times, and in experiments where reorientation of the organisms occurs, large-deviation theory should allow us to derive the probability distributions. We have not done this yet (except to examine the tails, as in [36]), but we can examine numerically whether the diffusive scaling is expected to hold for longer times.

To summarize the difference: in the diffusive scaling studies in this paper so far, we assumed that the number of reorientations t/τ was negligible because of the short times in the *Leptos et al.* experiments, which led to (32). The time-dependence thus entered through the path length $\lambda = Ut$ in (32) and in the computation of Δ_λ for the different times. Now that we allow reorientation to occur, we take λ to be the fixed full path length, and t/τ counts the number of reorientations. Figure 12 shows the results: a diffusive scaling is much less apparent, except in the Gaussian core where we expect the scaling to be present. We conclude that the scaling should disappear for longer times, when the swimmers undergo a few reorientations.

ACKNOWLEDGMENTS

The author thanks Bruno Eckhardt and Stefan Zammert for providing the digitized data from *Leptos et al.* The paper also benefited from discussions with Peter Mueller, Saverio Spagnolie, and Benedek Valko. This research was supported by NSF grant DMS-1109315.

-
- [1] T. J. Pedley and J. O. Kessler, *Annu. Rev. Fluid Mech.* **24**, 313 (1992).
 [2] E. Lauga and T. R. Powers, *Rep. Prog. Phys.* **72**, 096601 (2009).

- [3] A. J. Rothschild, *Nature* **198**, 1221 (1963).
- [4] H. Winet, G. S. Bernstein, and J. Head, *J. Reprod. Fert.* **70**, 511 (1984).
- [5] J. Cosson, P. Huitorel, and C. Gagnon, *Cell Motil. Cytoskel.* **54**, 56 (2003).
- [6] E. Lauga, W. R. DiLuzio, G. M. Whitesides, and H. A. Stone, *Biophys. J.* **90**, 400 (2006).
- [7] A. P. Berke, L. Turner, H. C. Berg, and E. Lauga, *Phys. Rev. E* **101**, 038102 (2008).
- [8] K. Drescher, K. Leptos, I. Tuval, T. Ishikawa, T. J. Pedley, and R. E. Goldstein, *Phys. Rev. Lett.* **102**, 168101 (2009).
- [9] C. Dombrowski, L. Cisneros, S. Chatkaew, R. E. Goldstein, and J. O. Kessler, *Phys. Rev. Lett.* **93**, 098103 (2004).
- [10] J. P. Hernandez-Ortiz, C. G. Dtolz, and M. D. Graham, *Phys. Rev. Lett.* **95**, 204501 (2005).
- [11] P. T. Underhill, J. P. Hernandez-Ortiz, and M. D. Graham, *Phys. Rev. Lett.* **100**, 248101 (2008).
- [12] P. T. Underhill and M. D. Graham, *Phys. Fluids* **23**, 121902 (2011).
- [13] D. Saintillan and M. J. Shelley, *Phys. Rev. Lett.* **99**, 058102 (2007).
- [14] A. Sokolov, R. E. Goldstein, F. I. Feldchtein, and I. S. Aranson, *Phys. Rev. E* **80**, 031903 (2009).
- [15] D. Saintillan and M. J. Shelley, *J. Roy. Soc. Interface* **9**, 571 (2012).
- [16] M. E. Huntley and M. Zhou, *Mar. Ecol. Prog. Ser.* **273**, 65 (2004).
- [17] W. K. Dewar, R. J. Bingham, R. L. Iverson, D. P. Nowacek, L. C. St. Laurent, and P. H. Wiebe, *J. Mar. Res.* **64**, 541 (2006).
- [18] E. Kunze, J. F. Dower, I. Beveridge, R. Dewey, and K. P. Bartlett, *Science* **313**, 1768 (2006).
- [19] K. Katija and J. O. Dabiri, *Nature* **460**, 624 (2009).
- [20] J. O. Dabiri, *Geophys. Res. Lett.* **37**, L11602 (2010).
- [21] A. M. Leshansky and L. M. Pismen, *Phys. Rev. E* **82**, 025301 (2010).
- [22] J.-L. Thiffeault and S. Childress, *Phys. Lett. A* **374**, 3487 (2010), arXiv:0911.5511.
- [23] A. Lorke and W. N. Probst, *Limnol. Oceanogr.* **55**, 354 (2010).
- [24] K. Katija, *J. Exp. Biol.* **215**, 1040 (2012).
- [25] A. W. Visser, *Science* **316**, 838 (2007).
- [26] M. C. Gregg and J. K. Horne, *J. Phys. Ocean.* **39**, 1097 (2009).
- [27] E. Kunze, *J. Mar. Res.* **69**, 591 (2011).
- [28] C. Noss and A. Lorke, *Limnol. Oceanogr.* **59**, 724 (2014).
- [29] T. Ishikawa, J. T. Locsei, and T. J. Pedley, *Phys. Rev. E* **82**, 021408 (2010).
- [30] H. Kurtuldu, J. S. Guasto, K. A. Johnson, and J. P. Gollub, *Proc. Natl. Acad. Sci. USA* **108**, 10391 (2011).
- [31] G. L. M. no, T. E. Mallouk, T. Darnige, M. Hoyos, J. Dauchet, J. Dunstan, R. Soto, Y. Wang, A. Rousselet, and E. Clément, *Phys. Rev. Lett.* **106**, 048102 (2011).
- [32] I. M. Zaid, J. Dunkel, and J. M. Yeomans, *J. Roy. Soc. Interface* **8**, 1314 (2011).
- [33] J. C. Maxwell, *Proc. London Math. Soc.* **s1-3**, 82 (1869).
- [34] C. G. Darwin, *Proc. Camb. Phil. Soc.* **49**, 342 (1953).
- [35] M. J. Lighthill, *J. Fluid Mech.* **1**, 31 (1956), corrigendum **2**, 311–312.
- [36] Z. Lin, J.-L. Thiffeault, and S. Childress, *J. Fluid Mech.* **669**, 167 (2011), <http://arxiv.org/abs/1007.1740>.
- [37] A. Morozov and D. Marenduzzo, *Soft Matter* **10**, 2748 (2014).
- [38] T. V. Kasyap, D. L. Koch, and M. Wu, *Phys. Fluids* **26**, 081901 (2014).
- [39] D. O. Pushkin and J. M. Yeomans, *Phys. Rev. Lett.* **111**, 188101 (2013).
- [40] D. O. Pushkin and J. M. Yeomans, *J. Stat. Mech.: Theory Exp.* **2014**, P04030 (2014).

- [41] J. Dunkel, V. B. Putz, I. M. Zaid, and J. M. Yeomans, *Soft Matter* **6**, 4268 (2010).
- [42] D. O. Pushkin, H. Shum, and J. M. Yeomans, *J. Fluid Mech.* **726**, 5 (2013).
- [43] X.-L. Wu and A. Libchaber, *Phys. Rev. Lett.* **84**, 3017 (2000).
- [44] K. C. Leptos, J. S. Guasto, J. P. Gollub, A. I. Pesci, and R. E. Goldstein, *Phys. Rev. Lett.* **103**, 198103 (2009).
- [45] M. J. Lighthill, *Comm. Pure Appl. Math.* **5**, 109 (1952).
- [46] J. R. Blake, *J. Fluid Mech.* **46**, 199 (1971).
- [47] T. Ishikawa, M. P. Simmonds, and T. J. Pedley, *J. Fluid Mech.* **568**, 119 (2006).
- [48] T. Ishikawa and T. J. Pedley, *J. Fluid Mech.* **588**, 437 (2007).
- [49] B. Eckhardt and S. Zammert, *Eur. Phys. J. E* **35**, 96 (2012).

Appendix A: Expected number of interactions for asynchronous turning

In this Appendix we compute exactly the expected number of interactions that a collection of swimmers will have with a particle. We assume that the swimmers have equal path lengths of swimming, but their relative phases are random. We refer to this as *asynchronous turning*. We do this in detail, which allows to get expressions that are valid even if the volume is finite.

A single swimmer moving for a time $0 \leq t < \tau$ has a probability $p_t = \mathbb{P}(\mathcal{H}_t)$ defined in (6) of having an interaction with the target particle. The expected number of events is thus $\langle M_t \rangle = p_t$ for $0 \leq t < \tau$. If the swimmer moves for a time $t = k\tau$, k a nonnegative integer, the total number of events is the sum of the events at each interval τ . The expected number of encounters for this swimmer is then

$$\langle M_t \rangle = kp_\tau + p_0, \quad t = k\tau. \quad (\text{A1})$$

Note that $\langle M_0 \rangle$ is nonzero, since a swimmer might start within a distance R of the target particle and so lead to an immediate interaction. If we multiply (A1) by the number of swimmers N , we will get the expected value for a collection of synchronous swimmers, which all turn at the same time. We can generalize (A1) to allow for any value of $t \geq 0$ by using the floor function $\lfloor \cdot \rfloor$:

$$\langle M_t \rangle = \lfloor t/\tau \rfloor p_\tau + p_{\Delta t}, \quad \Delta t = t - \lfloor t/\tau \rfloor \tau. \quad (\text{A2})$$

For asynchronous swimmers, we shall again consider a single swimmer, but we assume it has already started on a partial path before $t = 0$. For $t \geq \tau$, we write

$$t = \tau_0 + \tau k_{t,\tau_0} + \tau_1, \quad 0 \leq \tau_i < \tau, \quad (\text{A3})$$

where $k_{t,\tau_0} = \lfloor (t - \tau_0)/\tau \rfloor$ is the number of full paths traversed. The two τ_i pieces account for the partial paths traversed at the beginning and at the end of the motion. We take $\tau_0 \in [0, \tau)$ to be a uniformly-distributed random variable; τ_1 then follows from $\tau_1 = t - \tau_0 - \tau k_{t,\tau_0}$. The randomness of τ_0 de-synchronizes the swimmers, so that they do not all turn simultaneously.

Write $p_t = \alpha t + p_0$, where

$$\alpha = V_{\text{cyl}}(R, U)/V, \quad p_0 = V_{\text{sph}}(R)/V, \quad (\text{A4})$$

which can be read off from (6)–(7). The expected number of \mathcal{H}_t events is

$$\begin{aligned} \langle M_t \rangle &= \langle p_{\tau_0} + k_{t,\tau_0} p_\tau + p_{\tau_1} \rangle = \langle \alpha(\tau_0 + \tau k_{t,\tau_0} + \tau_1) + (2 + k_{t,\tau_0}) p_0 \rangle \\ &= \alpha t + (2 + \langle k_{t,\tau_0} \rangle) p_0. \end{aligned}$$

To compute $\langle k_{t,\tau_0} \rangle$, let $t/\tau = \ell + \delta$, $\ell = \lfloor t/\tau \rfloor$, and $\delta \in [0, 1)$. Then $\langle k_{t,\tau_0} \rangle = \langle \lfloor (t - \tau_0)/\tau \rfloor \rangle = \ell + \langle \lfloor \delta - (\tau_0/\tau) \rfloor \rangle$, with $|\delta - (\tau_0/\tau)| < 1$, and

$$\langle \lfloor \delta - (\tau_0/\tau) \rfloor \rangle = \frac{1}{\tau} \int_0^\tau [\delta - (\tau_0/\tau)] d\tau_0 = \int_0^1 [\delta - \xi] d\xi = \int_\delta^1 (-1) d\xi = \delta - 1.$$

Thus,

$$\langle k_{t,\tau_0} \rangle = \ell + \delta - 1 = (t/\tau) - 1, \quad (\text{A5})$$

and we finally conclude

$$\langle M_t \rangle = (\alpha\tau + p_0) (t/\tau) + p_0 = p_\tau (t/\tau) + p_0. \quad (\text{A6})$$

For $t < \tau$, the random variable τ_0 can take a value smaller or larger than t . In the first case we have two interactions since the swimmer will end its first path before time t . In the second we have one interaction. We thus have

$$\langle M_t \rangle = \frac{1}{\tau} \left(\int_0^t (p_{\tau_0} + p_{t-\tau_0}) d\tau_0 + \int_t^\tau p_t d\tau_0 \right), \quad t < \tau, \quad (\text{A7})$$

which gives the same answer as (A6), so that form is valid for all $t \geq 0$. The extra p_0 at the end of (A6) arises from the possibility of swimmers starting inside the interaction sphere at $t = 0$. This expression coincides with (A1) (the synchronous case) when $t = k\tau$, but it is valid for any $t \geq 0$ because of the averaging over the random phase.

We can also compute the variance exactly. For a single synchronous swimmer starting its path at $t = 0$,

$$\text{Var } M_t = p_t(1 - p_t), \quad t < \tau. \quad (\text{A8})$$

For an asynchronous swimmer, we have for $t \geq \tau$

$$\begin{aligned} \text{Var } M_t &= \langle p_{\tau_0}(1 - p_{\tau_0}) + k_{t,\tau_0} p_\tau(1 - p_\tau) + p_{\tau_1}(1 - p_{\tau_1}) \rangle \\ &= \langle M_t \rangle - \langle p_{\tau_0}^2 + k_{t,\tau_0} p_\tau^2 + p_{\tau_1}^2 \rangle \leq \langle M_t \rangle. \end{aligned}$$

We need to compute the expectation value of this over τ_0 . This is a slightly tedious calculation which we do not present; the final result is

$$\text{Var } M_t = p_\tau(1 - p_\tau) (t/\tau) + p_0(1 - p_0) + \frac{1}{3}(\alpha\tau)^2, \quad t \geq \tau. \quad (\text{A9})$$

For $t < \tau$

$$\text{Var } M_t = \frac{1}{\tau} \left(\int_0^t (p_{\tau_0}(1 - p_{\tau_0}) + p_{t-\tau_0}(1 - p_{t-\tau_0})) d\tau_0 + \int_t^\tau p_t(1 - p_t) d\tau_0 \right), \quad t < \tau, \quad (\text{A10})$$

which gives

$$\text{Var } M_t = p_t(1 - p_t) + p_0(1 - p_0)(t/\tau) + \frac{1}{3}(\alpha t)^2(t/\tau), \quad t < \tau. \quad (\text{A11})$$

When p_t is small we recover $\text{Var } M_t \simeq \langle M_t \rangle$. The other terms (quadratic in p_t and α) are finite-volume corrections.

For N swimmers, because we are still summing the number of displacements, the net result is to multiply the expected number of events (A6) and its variance (A9) by N . After substituting the value of α and p_0 from (A4), then using $n = N/V$, we obtain equations (8) and (9).